Organic & Biomolecular Chemistry

Cite this: *Org. Biomol. Chem.*, 2012, **10**, 7334

www.rsc.org/obc

PAPER

Towards β-selectivity in functional estrogen receptor antagonists†

Jose Juan Rodríguez,[a] Kamila Filipiak,[a,b] Maciej Maslyk,[a,b] Jakub Ciepielski,[a,c] Sebastian Demkowicz,[a,d] Sonia de Pascual-Teresa,[e] Sonsoles Martín-Santamaría,*[a] Beatriz de Pascual-Teresa[a] and Ana Ramos*[a]

Received 1st June 2012, Accepted 11th July 2012
DOI: 10.1039/c2ob26062j

Based on the benzo[*b*]naphtho[1,2-*d*]furan and benzo[*b*]naphtho[1,2-*d*]thiophene frameworks, a series of ligands with different basic side chains (BSCs) has been synthesized and pharmacologically evaluated. Also, their binding modes have been modelled using docking techniques. It was found that the introduction of a BSC in these systems brings about a decrease of affinity for both estrogen receptors α and β in an *in vitro* competitive binding assay. However, two full antagonists of the estrogen receptor β (**9c** and **9f**) have been discovered, with potency in the low micromolar concentration in a cell-based luciferase reporter assay, and completely devoid of activity against the α receptor at the same concentration range. Differences in the ERα/ERβ binding modes have also been rationalized with the help of molecular modelling techniques. This interesting functional profile could be used to elucidate the physiological role of each ER subtype.

Introduction

The biological actions of estrogens are manifested through two genetically distinct estrogen receptors (ERα and ERβ) that display nonidentical expression patterns in target tissues. Interesting differences have been found in the physiological role of both receptor subtypes. ERα is predominantly involved in the development and function of the mammary gland and uterus, and in the maintenance of metabolic and skeletal homeostasis. ERβ has more pronounced effects on the central nervous system and on cellular hyperproliferation.[1]

Since the discovery of ERβ in 1996, compounds that are selective in activating or inhibiting both ER subtypes are intensively sought after.[2] The data obtained suggest that the discovery of compounds that selectively bind ERα or ERβ is of great interest for the development of more efficient drugs for the treatment of several disorders, such as cancer, cardiovascular disease, multiple sclerosis and Alzheimer's disease.[3,4] The use of the ERα selective agonist propylpyrazoletriol (PPT) (Fig. 1) has shown that several classical estrogen-induced tissue responses can be effectively evoked *via* ERα alone.[5] On the other hand, the design of highly ERβ selective ligands has proved to be quite challenging, and several groups have reported attempts to design this kind of compound using different scaffolds. The highly ERβ selective agonist ERB-041 (Fig. 1) has been used to demonstrate that this receptor may be a useful target for certain inflammatory diseases. This compound has a dramatic beneficial effect in the HLA-B27 transgenic model of inflammatory bowel disease and the Lewis rat adjuvant-induced arthritis model, while it is inactive in several classic models of estrogen action.[6] Other non-steroidal scaffolds which have been developed as ERβ ligands are diarylpropanenitriles,[7] 2-phenylnaphthalenes,[8,9] and phenyl-2*H*-indazoles.[10]

Interestingly, some substituted tetrahydrochrysene ligands such as *cis*-(*R*,*R*)-diethyl (THC) (Fig. 1) have been described as potent agonists on ERα, but more potent antagonists on ERβ,[11,12] in contrast with tamoxifen and raloxifene which are partial antagonists on both ERα and ERβ (Fig. 1). The structure of these ERβ antagonists is also different from the structure of tamoxifen and raloxifene, where the bulky basic side chain (BSC) is responsible for their antagonist activity through the blockage of the ER helix-12 movement by interaction with Asp351 carboxylate (ERα numbering).[13] Crystallographic structures of the ERα ligand binding domain (LBD) bound to both THC and a fragment of the transcriptional coactivator GRIP1, and ERβ LBD bound to THC show that this compound antagonizes ERβ through a novel mechanism termed "passive

[a]*Departamento de Química, Facultad de Farmacia, Universidad CEU San Pablo, 28668-Boadilla del Monte, Madrid, Spain. E-mail: aramgon@ceu.es, smsantamaria@ceu.es; Fax: (+34) 913510496; Tel: (+34) 913724796*
[b]*Department of Molecular Biology, Faculty of Mathematics and Natural Sciences, The John Paul II Catholic University of Lublin, 20-718 Lublin, Poland*
[c]*Department of Environmental Biochemistry and Chemistry, Faculty of Mathematics and Natural Sciences, The John Paul II Catholic University of Lublin, 20-718 Lublin, Poland*
[d]*Department of Organic Chemistry, Gdansk University of Technology, 11/12 G. Narutowicza St., 80-233 Gdańsk, Poland*
[e]*Institute of Food Science, Food Technology and Nutrition (ICTAN), Spanish National Research Council (CSIC), José Antonio Novais 10, 28040-Madrid, Spain*

† Electronic supplementary information (ESI) available: δ_H and δ_C NMR spectra of compounds **5b**, **6b**, **7b**, **8a–j**, **9a–j**, **10** and **11**. Data from docking calculations and MD simulations. See DOI: 10.1039/c2ob26062j

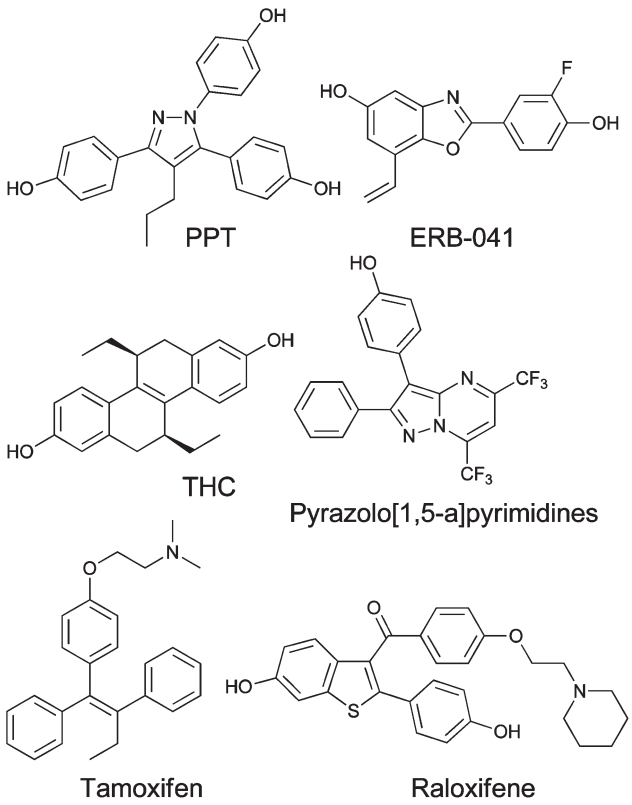

Fig. 1 Chemical structures of some known ERα- or ERβ-selective ligands and tamoxifen and raloxifene.

antagonism".[14] Other series of ERβ-selective modulators based on a 1,3,5-triazine scaffold, that behave as ERα partial agonists and ERβ antagonists, have been identified.[15]

However, there are few examples of compounds that are more potent antagonists of ERβ than of ERα.[2] Pyrazolo[1,5-*a*]pyrimidines (Fig. 1) possess this new profile: they are passive on both ERs, with a distinct potency selectivity in favor of ERβ. In a recent structure-based virtual screening, one antagonist for both subtypes, showing significant selectivity for ERβ, was discovered, which showed inhibitory activities on the proliferation of the MCF-7 cell line.[16]

Compounds acting as ERβ antagonists are interesting to probe the biology of this receptor subtype, and they can be useful to understand the role that the ERβ play in several types of cancers such as prostate, colon and lung cancers, where it is the predominant ER subtype.[4]

With the purpose of extending the available scaffolds useful for the design of new selective estrogen receptor modulators (SERMs), we initiated a program directed to the synthesis of tetracyclic systems containing an oxygen or sulphur atom, and an additional cyano substituent, that could be used to introduce the appropriate basic chains (Fig. 2). We found that compounds **2** and **3**, with modest selectivity for ERβ in a scintillation proximity assay, behave as ERβ agonists and ERα antagonists,[17] and present interesting antitumor activity against two pancreatic cell lines.[18]

The aim of the present study is to transform these ERβ agonists into antagonists by the introduction of the BSCs present in tamoxifen, raloxifene and other antagonists described in the literature. We have evaluated the ERα and ERβ binding affinities

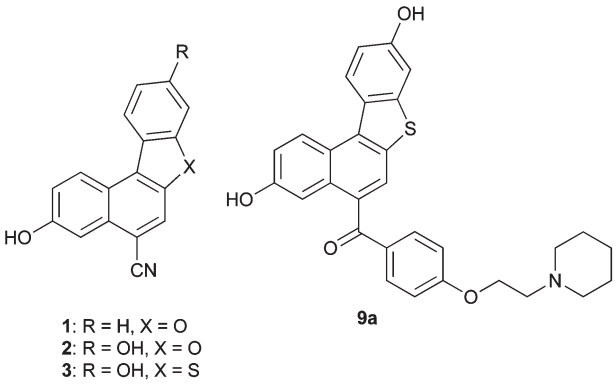

Fig. 2 Chemical structures of compounds **1–3** and **9a**.

of the synthesized compounds and studied the transcriptional efficacy and MCF-7 antiproliferative activity of the most interesting of these. The most active compounds in the series behave as ERβ-selective functional antagonists, which make them interesting tools to elucidate the biological effects of this receptor subtype. Molecular modelling studies have helped to rationalize these findings.

Results and discussion

Chemistry

In our previous work we described the synthesis of benzonaphthofurans and benzonaphthothiophenes **1–3**, and we studied their affinity towards both estrogen receptors α and β.[17] These compounds were designed bearing a cyano group in their structure to allow their transformation into antagonists by the introduction of the appropriate BSC. In fact, a basic side chain was introduced to give **9a** (Table 1) *via* the five step synthetic pathway depicted in Scheme 1, demonstrating that these are suitable scaffolds for the design of potential new SERMs.

In this paper we have extended this study to the synthesis of compounds **9b–9j** (Table 1) following the same synthetic pathway. Thus, compound **5b** was synthesized by reacting **4b** with 4-fluorophenylmagnesium bromide. Treatment of **5b** with BBr_3 gave **6b**, which was transformed into the benzyl-protected derivative **7b** by reaction with benzyl bromide in the presence of K_2CO_3. Both **7a**[17] and **7b** were useful intermediates for the synthesis of the final compounds **9**, through nucleophilic aromatic substitution of the fluorine atom by the corresponding alcohol or amine using NaH and K_2CO_3 respectively as a base, followed by deprotection of the hydroxyl groups. Deprotection using H_2 and Pd/C 5% under different conditions of pressure and temperature gave poor yields of the deprotected compound.[17]

However, the use of black palladium and ammonium formate as the source of hydrogen gave excellent yields of compounds **9**, which were converted to the corresponding hydrochloride salts to be tested in the biological assays.

Molecular modelling

Docking studies. Docking studies were performed on selected final compounds (**9a–9c** and **9f–9j**, Table 1) with the aim of

Table 1 Chemical structure and yields in the synthesis of compounds **8a–j** and **9a–j**

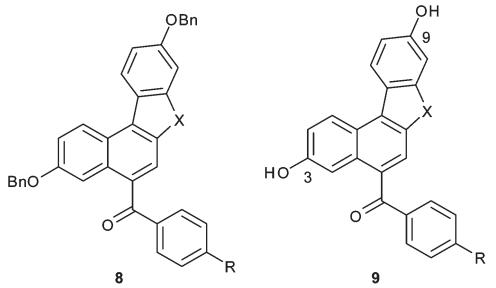

Comp.	X	R	Yield **8**/**9** (%)
8a/**9a**	S	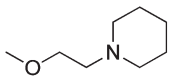	85/90
8b/**9b**	S	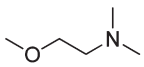	77/59
8c/**9c**	S	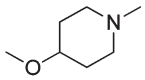	76/75
8d/**9d**	S	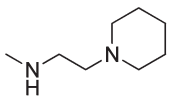	85/90
8e/**9e**	S	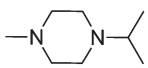	85/99
8f/**9f**	O	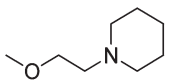	96/85
8g/**9g**	O	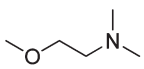	93/95
8h/**9h**	O	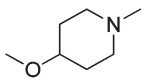	85/71
8i/**9i**	O	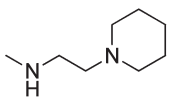	85/87
8j/**9j**	O	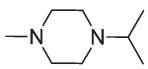	85/79

studying how different BSCs modulate the interaction with the receptor. In order to explore different binding modes of the ER in complex with agonists and antagonists, several crystallographic structures were used: ERα in complex with estradiol (PDB 1A52), raloxifene (PDB 1ERR), genistein (PDB 1X7R) and 4-hydroxytamoxifen (PDB 3ERT), and ERβ in complex with genistein (PDB 1X7J), THC (PDB 1L2J) and 4-hydroxytamoxifen (PDB 2FSZ). Two different docking programs were used, AutoDock4 and Glide, to compare the results (see ESI† for docking energies).

Although compound **6b**, with a short side chain, is a synthetic intermediate, we were also interested in the study of its binding mode, so it was considered in the docking calculations, as well as estradiol, genistein and 4-hydroxytamoxifen as reference compounds to validate the computational protocols. Overall results are here presented; focusing on the different features found in the binding, therefore relevant biological information can be inferred for the series of compounds.

For compound **6b**, in general, the results of the docking studies predicted best binding poses towards ERβ, in terms of docking energy (for example, the value of the Glide score was ERα = 7.6 kcal mol^{-1}; ERβ = −10.0 kcal mol^{-1}), and were in agreement with the experimental data of RBA (relative binding affinity). Hydrogen bonds are established between the HO-9 group with Arg346 and the carbonyl group of Leu339, between the HO-3 group with Thr299, and between the carbonyl group and the NH of His475 (Fig. 3). The side chain occupies a hydrophobic region delimited by residues Leu380, Ile373 and Phe377. An alternative binding mode is also observed in which the aromatic ring provides a stacking interaction with the imidazole ring of His475. The docking calculations in ERα predicted a binding mode in which the two hydroxyl groups establish hydrogen bonds with Arg394–Glu353, and with Thr347, while the side chain establishes a stacking interaction with the imidazole from His524. As expected, no binding pose with interactions with ERα Asp351 (ERβ Asp303) was predicted (Fig. 3).

For compounds **9a–9c** and **9f–9j**, docking studies allowed the identification of binding poses in agreement with the obtained affinity values (Table 2), noticing key interactions of the tetracycle into the LBD similar to those for genistein and 4-hydroxytamoxifen: hydroxyl groups establish hydrogen bonds with Glu353, Arg394 and/or the Leu387 carbonyl group in one of the

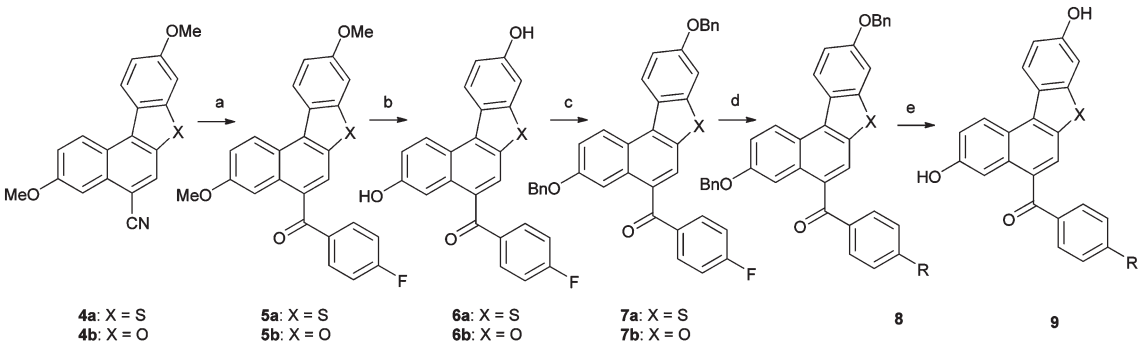

Scheme 1 Reaction conditions for the synthesis of compounds **8** and **9**. (a) 4-Fluorophenylmagnesium bromide, THF reflux for 24 h, 98% for **5b**; (b) BBr_3, DCM, 95%; (c) benzyl bromide, K_2CO_3, EtOH, 95% for **6b**; (d) RH/NaH, DMF for **8a–c** and **8f–h** or RH/K_2CO_3, DMF for **8d,e** and **8i,j**; (e) H_2, black palladium, ammonium formate.

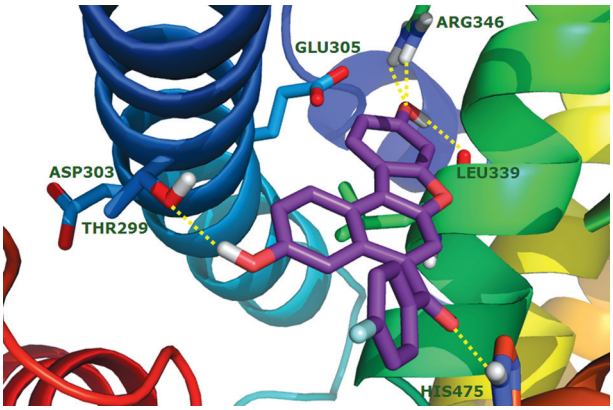

Fig. 3 Docked binding mode obtained with Glide for compound **6b** in ERβ.

Table 2 Estrogen receptor relative binding affinity (RBA) and IC_{50} for compounds **2**, **3**, **6b**, **9a–c**, **9f**, **9i**, **9j**, **10** and **11**

Ligand	ERα IC_{50}[a] (μM)	ERβ IC_{50}[a] (μM)	RBA (ERα)	RBA (ERβ)	β/α ratio
2	7.02	1.76	0.128	0.39	3.05
3	30.83	6.0	0.029	0.115	3.93
6b	68.0	25.0	0.013	0.027	2.08
9a	>100	49.27	—	0.013	—
9b	21.40	25.29	0.042	0.027	0.65
9c	12.78	18.07	0.07	0.038	0.54
9f	24.92	12.19	0.036	0.056	1.56
9h	7.46	7.38	0.120	0.093	0.77
9i	34.8	>50	0.025	—	—
9j	11.66	7.06	0.077	0.097	1.26
10	NA	NA	NA	NA	—
11	23.91	31.59	0.037	0.021	0.56

[a] Values are an average of at least 3 experiments with typical standard errors below 15%; NA – not achieving binding at the assayed concentration.

Table 3 Agonistic and antagonistic profile and antiproliferative activities of selected compounds

	Agonistic activity (EC_{50}) (μM)		Antagonistic activity (IC_{50})[a] (μM)		
Ligand	ERα	ERβ	ERα	ERβ	MCF-7 IC_{50}[b] (μM)
6b	Weak	—	—	0.592 ± 0.04	2.42 ± 0.38
9c	—	—	—	0.148 ± 0.0068	3.34 ± 0.71
9f	—	—	—	0.183 ± 0.007	2.25 ± 0.43

[a] Experimental values represent the average of 2 experiments performed in triplicate along with standard deviation (SD) between assay values. [b] Experimental values represent the average of 3 experiments performed in quintuplicate along with standard deviation (SD) between assay values.

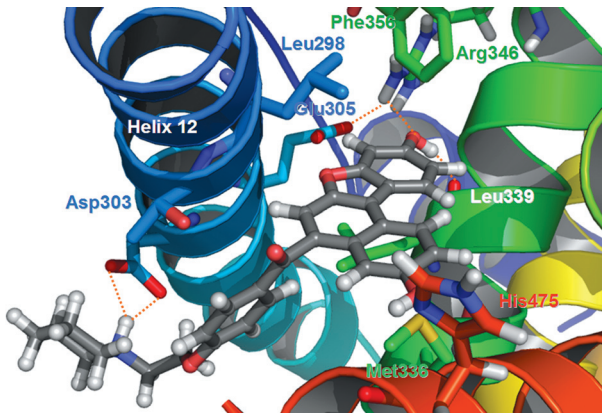

Fig. 4 Docked binding mode obtained with Glide for compound **9f** in ERβ.

binding site ends, and with His524 in the other end (ERα numbering).

Careful study of the results reveals some differences depending on the nature of the tetracycle. For benzothiophene derivatives (**9a**, **9b** and **9c**), only docked binding poses into ERβ showed the characteristic interactions together with one interaction of the BSC with Asp303, putting forward the possibility of antagonist behaviour. Remarkably, compound **9c** clearly showed ERβ selective antagonism in the functional characterization studies (Table 3).

Regarding benzofuran derivatives, for compounds **9g**, **9h** and **9i**, several binding poses were predicted without remarkable ERα/ERβ differences in terms of energy, either with AutoDock or Glide. Although in the case of ERβ a larger number of binding poses were obtained, the theoretical binding energies were very similar, not pointing to a clear prediction of selectivity for these three compounds. However, this was not the case for the other benzofuran compounds, **9j** and **9f**. It is worth mentioning that for compound **9j**, both docking programs only led to binding solutions in ERβ. For compound **9f** only ERβ binding solutions were predicted by AutoDock, while Glide showed similar results in both receptors (Fig. 4). These results could point towards a theoretical ERβ selectivity for **9j** and **9f**. As will be shown below, affinity data confirmed these predictions. Moreover, both compounds were shown to be ERβ selective in the functional characterization studies. Additional MD simulations were performed on the ERβ–**9f** complex (see below).

Superimposition of docked poses of compound **9f** and the thioderivative **9a** led to the observation of a shift of **9a** relative to the position occupied by **9f** within the LBD, which is justified by repulsion of the sulphur atom with an Ala302 side chain. This shifting also prevents the hydrogen bond formation between the OH-9 group and Arg346, and might explain the poor ERβ affinity found for this compound. The larger volume of the thioligand and this repulsion could also justify that the docking studies did not provide any binding solution in the ERα for compound **9a**. A similar repulsive interaction, involving the sulphur atom, was observed in the thioderivative **3**,[17] thus accounting for the ERβ selectivity. It is worth mentioning that for compounds **9a**, **9c** and **9j** docking results were only obtained in the ERβ. In the agonism/antagonism profile assays, compound **9c** showed an IC_{50} value of 0.148 ± 0.0068 μM as an ERβ antagonist (see below), which is in agreement with the prediction.

Regarding the nature of the side chains, docking studies led to better results for compounds with flexible chains in terms of

energy, number of binding poses and geometry of the interaction (data not shown), highlighting the interaction of the protonated BSC nitrogen with the Asp303 carboxylate from helix-12. However, it is important to mention that this interaction was also observed in scarce solutions for the piperidine derivatives. In any case, the best docking results corresponded to the ERβ binding.

Molecular dynamics simulations

Prompted by the experimentally found ERβ selectivity for compound **9f**, molecular dynamics simulations were performed on the ERβ–**9f** complex. The starting structure was obtained from the docking studies (see Experimental). Initially, during the equilibration period, positional restraints to α-carbon atoms were applied, together with a distance restraint to keep the interaction between the Asp303 carboxylate moiety and the piperidinium NH group. Then, restrictions were gradually lowered until no restriction was applied. As a further step, two independent MD simulations were then continued: the first one maintained the COO···HN distance restraint during the initial 500 ps followed by 1 ns of simulation with no restriction, while the second one was run without any restrictions during 2 ns. The analysis of the results showed that the complex remained fairly stable during the simulations, maintaining a variety of stabilizing interactions within the LBD. However, in both cases, the above mentioned salt bridge was lost within a few ps when the corresponding restriction was removed. Indeed, it was observed that the Asp303 side chain suffers a conformational change, exposing the carboxylate moiety to the solvent (see ESI†). Then, it fluctuates during the rest of the simulation time, establishing transient hydrogen bonds with water molecules. In any case, rotation of the helix-12 would be prevented due to the stability of the receptor–ligand complex, and to the presence of the BSC.

Estrogen receptor binding affinity

The RBAs of compounds **6b**, **9a–c**, **9f**, **9h–j**, **10** and **11** were determined in an *in vitro* competitive binding assay following a reported method[19] with some modifications. To compare the affinity of these compounds with their parent tetracyclic analogues lacking the basic chain, we have also measured the RBAs of **2** and **3** in this assay. Table 2 shows a summary of the results obtained (E_2 has an RBA of 100%). Under these conditions, **2** was found to have the highest RBA for ERα (0.128) and ERβ (0.39), with a slight selectivity for ERβ (β/α = 3.05), which is in agreement with our previously published affinity results using a scintillation proximity assay.[17] In the case of the benzonaphthofuran series, compound **3** showed less affinity than the oxygen analogue **2**, with an RBA of 0.029 for ERα and 0.115 for ERβ, and similar selectivity (β/α = 3.05). The RBA values for **6b** and **9** vary from 0.013 to 0.120 for ERα and from 0.027 to 0.097 for ERβ, showing that the introduction of a short side chain (compound **6b**) or a BSC brings about a decrease in the affinity of this type of compound and a decrease in selectivity. It should be noted that under our experimental conditions the binding between estradiol and ERα is more effective than that of ERβ. Since data are expressed as a percentage related to estradiol this means that the actual ratios ERβ/ERα may be even higher than calculated.

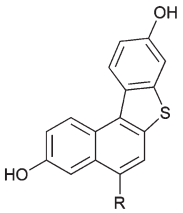

10: R = COOH
11: R = COOMe

Fig. 5 Chemical structures of compounds **10** and **11**.

In our previous work[17] on ER ligands based on novel tetracyclic scaffolds, the most interesting result was found for compounds **2** and **3**, which behaved as ERβ agonists and ERα antagonists, and presented a 3.5-fold higher affinity toward ERβ. This result was rationalized, based on molecular modelling studies, by an additional interaction between the cyano group present in these compounds and ERβ Thr299, not present in the docked complex with ERα. In an attempt to improve the affinity and selectivity of this type of compound, and to get more information on the importance of this interaction, we carried out docking studies of twelve analogues of **2** and **3**, by substituting the cyano group by functional groups able to establish hydrogen bonds with Thr299.

These functional groups were COOH, $COOCH_3$, $CONH_2$, CHO, $COCH_3$, and CH_2OH, and the docking was carried out in both alpha and beta ERs, in agonist (PDB codes 1X7E and 1YYE) and antagonist (PDB codes 1ERR and 1L2J) conformations. Docking results were able to highlight proper interactions with Thr299 in the antagonist conformation of ERβ, without showing remarkable differences between furan/thiophene analogues. Finally, compounds **10** and **11** (Fig. 5) were synthesized to test their biological behaviour. The competitive binding assay showed that the substitution of the cyano group by a carboxylic acid (**10**) brings about a complete loss of affinity. In the case of ester **11**, a decrease in the affinity for ERβ is observed, while the affinity for ERα is little affected.

In vitro functional activity of selected ER ligands

With the purpose of characterizing the agonist/antagonist profile of these compounds, we have selected compounds **6b** and **9f** as representative ERβ binders and **9c** as a representative ERα binder. The agonistic and antagonistic activities of the compounds were evaluated using a commercially available cell-based assay (INDIGO Bioscience's ER Reporter Assay), which allows quantifying functional activities of the tested compounds, against ERα and ERβ. The system utilizes non-human mammalian cells engineered to provide constitutive high-level expression of ERα and ERβ. Additionally, these cells contain either the ERα or ERβ-responsive luciferase reporter gene. Thus, quantification of luciferase activity provides a surrogate measure of ERα and ERβ activation in the treated reporter cells. Although the compounds possessed only low RBAs, they proved to have a significant antagonistic effect on ERβ, and almost no effect on ERα. Compound **6b** showed antagonistic activity in ERβ, already pointing at the potential of benzonaphthofuran **3** to be

converted into an ERβ antagonist through the introduction of the BSC.

Interestingly, when a BSC was introduced, as in **9c** and **9f**, full ERβ antagonists were obtained, with an IC_{50} of 0.183 ± 0.007 and 0.148 ± 0.0 068 μM, respectively, while they were completely devoid of activity against the α receptor at the same concentration range. These results are in agreement with the predicted lack of interaction of the BSC with ERα Asp351 carboxylate for most of the here reported compounds (see docking studies). Thus, although these ligands possessed low RBAs, and did not show any significant subtype preference in binding assays, they proved to share significant degrees of antagonism on ERβ. Given the limited number of examples of ERβ-selective antagonists available,[4] these compounds could be used as potential molecular probes to differentiate the biological roles of both ER subtypes.

In vitro antiproliferative activity

Compounds **6b**, **9c** and **9f**, characterized as full antagonists at low micromolar concentration, were selected for the assessment of antiproliferative potencies on the human MCF-7 breast cancer line (Table 3). All of them displayed activity at higher concentrations, with IC_{50} within the range of 2.25 to 3.34 μM. This result is in accordance with their antagonistic character. The modest antiproliferative activity observed was expected, as MCF-7 is a human breast cancer cell line showing a low level of ERβ expression.

Conclusions

We have used the benzo[*b*]naphtho[1,2-*d*]furan and benzo[*b*]-naphtho[1,2-*d*]thiophene systems, previously described by us as selective β-agonists,[17] to generate a series of antagonists by the introduction of the BSCs present in tamoxifen, raloxifene and other antagonists described in the literature. The antagonism is thus produced through the establishment of an interaction between this BSC and Asp303 carboxylate (ERβ numbering), blocking the ER helix-12 movement. Docking studies on our compounds have pointed towards a clearly preferred ERβ binding, and have allowed proposing binding modes exhibiting the interaction of the BSC and Asp303 carboxylate from helix-12. Among these novel ligands, compounds **9c** and **9f** presented a promising profile, with low micromolar activity as ERβ antagonists in a cell-based functional assay, and no activity in ERα at the same concentration range.

There are few examples of ligands with this β-selective antagonistic profile. The ability of these compounds to annul the estrogen action through ERβ, without having any effect on its activity through ERα, could be used to differentiate the biological roles of both ER subtypes.

Experimental

General methods

Melting points (uncorrected) were determined on a Stuart Scientific SMP3 apparatus. Infrared (IR) spectra were recorded with a Perkin-Elmer 1330 infrared spectrophotometer. ^1H and ^{13}C NMR were recorded on a Bruker 300-AC instrument. Chemical shifts (δ) are expressed in parts per million; coupling constants (J) are in Hertz. Mass spectra were run on a Bruker Esquire 3000 spectrometer. Thin-layer chromatography (TLC) was run on Merck silica gel 60 F-254 plates. Unless stated otherwise, starting materials used were high-grade commercial products. Compounds **9a–c**, **9f** and **9h–j** were tested as hydrochlorides and their purities were determined by HPLC on an Agilent 1100 HPLC system with a UV detector, using a C18 reversed-phase Discovery column (15 × 4.6 mm ID, 5 μm), eluting with an isocratic pH 7 phosphate buffer–methanol (80 : 20 v/v) mobile phase.

(3,9-Methoxybenzo[*b*]naphtho[1,2-*d*]furan-5-yl)(4-fluorophenyl)-methanone 5b. To a solution of **4b**[17] (0.98 g, 3.23 mmol) in THF (20 cm^3) was added a solution of 4-fluorophenylmagnesium bromide (65 cm^3, 1 M in THF, 65 mmol) at RT, and the mixture was refluxed for 24 h. After cooling, HCl 3 N (20 cm^3) was added to the crude, and a red solid, which was characterized as the imine of **5b**, precipitated. The solid was isolated by filtration and after adding HCl 3 N (125 cm^3), the suspension was refluxed for 48 h. The new yellow precipitate formed was extracted with DCM (3 × 20 cm^3) and the organic extracts were washed with brine, dried ($MgSO_4$), and evaporated to give **5b** (1.26 g, 98%) as a yellow solid, mp 170–171 °C; ν_{max} (KBr)/cm^{-1} 1620; δ_H (300 MHz, $CDCl_3$) 3.68 (3 H, s, OMe), 3.93 (3 H, s, OMe), 7.07 (1 H, dd, *J* 2.4, 8.8, ArH), 7.15–7.20 (3 H, m, ArH), 7.39 (1 H, dd, *J* 2.4, 9.3, ArH), 7.76 (1 H, d, *J* 2.4, ArH), 7.81 (1 H, s, ArH), 7.94 (2 H, d, *J* 8.8, ArH), 8.09 (1 H, d, *J* 8.8, ArH) and 8.36 (1 H, d, *J* 8.8, ArH); δ_C (75.4 MHz; $CDCl_3$) 55.1, 55.6, 96.3, 105.7, 112.1, 115.4, 115.6, 115.7, 117.1, 119.6, 121.2, 122.6, 123.9, 125.0, 129.7, 132.1, 132.9, 133.0, 135.0, 135.02, 150.6, 157.3, 158.2, 159.8, 163.9, 167.3 and 195.9; EIMS (*m*/*z*) 400 $[M]^+$.

(3,9-Dihydroxybenzo[*b*]naphtho[1,2-*d*]furan-5-yl)(4-fluorophenyl)-methanone 6b. To a solution of **5b** (0.8 g, 2 mmol) in dry DCM (20 cm^3) was added BBr_3 (40 cm^3, 1 M in DCM, 40 mmol) at 0 °C. The mixture was stirred in a sealed tube at 70 °C for 48 h. After cooling to room temperature, the crude reaction mixture was quenched carefully with ice, water and 1 N HCl. The aqueous layer was extracted with AcOEt (3 × 50 cm^3) and the combined organic extracts were washed with saturated aqueous $NaHCO_3$ and brine, dried ($MgSO_4$) and concentrated to dryness to give **6b** (0.71 g, 95%) as a solid, mp 224–225 °C; ν_{max} (KBr)/cm^{-1} 1595 and 3300; δ_H (300 MHz, MeOD) 6.95 (1 H, dd, *J* 2.4, 8.6, ArH), 7.00–7.04 (2 H, m, ArH), 7.09–7.14 (2 H, m, ArH), 7.25 (1 H, dd, *J* 2.4, 9.2, ArH), 7.59 (1 H, s, ArH), 7.66–7.71 (2 H, m, ArH), 8.15 (1 H, d, *J* 8.6, ArH) and 8.45 (1 H, d, *J* 9.2, ArH); δ_C (75.4 MHz; MeOD) 99.3, 109.8, 113.5, 116.4, 116.8, 117.7, 120.3, 123.6, 124.2, 126.6, 130.5, 131.9, 132.1, 135.5, 136.0, 136.02, 152.5, 155.8, 158.8, 159.3, 164.4, 167.8 and 179.1; EIMS (*m*/*z*) 395 $[M + Na]^+$; HPLC purity: 96.52.

(3,9-Dibenzyloxybenzo[*b*]naphtho[1,2-*d*]furan-5-yl)(4-fluorophenyl)methanone 7b. A solution of **6b** (0.5 g, 1.34 mmol), K_2CO_3 (3.2 g, 23 mmol) and benzyl bromide (0.96 cm^3, 8.1 mmol) in EtOH (3 cm^3) was refluxed for 24 h. The reaction

was then diluted with AcOEt, washed with water and brine, dried ($MgSO_4$) and evaporated to dryness. The residue was purified by flash column chromatography using hexane–AcOEt (9 : 1) as an eluent to give **7b** (0.72 g, 82%) as a yellow solid, mp 155–157 °C; ν_{max} (KBr)/cm^{-1} 1590 and 3020; δ_H (300 MHz, $CDCl_3$) 5.11 (2 H, s, CH_2O), 5.12 (2 H, s, CH_2O), 7.14–7.20 (3 H, m, ArH), 7.36–7.50 (12 H, m, ArH), 7.82–7.86 (2 H, m, ArH), 7.93–7.95 (2 H, m, ArH), 8.27 (1 H, d, *J* 7.8, ArH) and 8.56 (1 H, d, *J* 8.8, ArH); δ_C (75.4 MHz; $CDCl_3$) 69.8, 70.3, 97.4, 106.9, 112.7, 115.4, 115.5, 115.7, 117.3, 119.9, 121.1, 122.7, 124.0, 125.0, 127.6, 127.9, 128.1, 128.5, 129.6, 132.2, 132.9, 133.0, 134.8, 134.9, 136.3, 136.5, 150.76, 156.5, 158.1, 158.8, 163.9, 167.3 and 195.9; EIMS (*m*/*z*) 553 $[M + H]^+$.

(3,9-Dibenzyloxybenzo[*b*]naphtho[1,2-*d*]thiophen-5-yl)(4-[2-(*N*,*N*-dimethyl)ethoxy]phenyl)methanone 8b. To a solution of 2-(dimethylamino)ethanol (0.31 g, 3.5 mmol) in DMF (5 cm^3) was added NaH (0.08 g, 3.5 mmol) and the mixture was stirred at RT for 30 min. Then **7a**[17] (0.1 g, 0.18 mmol) was added, and the stirring was continued for 6 h. To the solution was added water, and the aqueous layer was extracted with AcOEt, washed with brine, dried ($MgSO_4$) and evaporated. The residue was purified by flash column chromatography using AcOEt–MeOH (9 : 1) as an eluent to give **8b** (0.086 g, 77%) as a yellow oil; ν_{max} (KBr)/cm^{-1} 1597 and 2931; δ_H (300 MHz, $CDCl_3$) 2.37 (6 H, s, $2CH_3$), 2.75–2.84 (2 H, m, CH_2N), 4.11–4.20 (2 H, m, CH_2O), 5.08 (2 H, s, CH_2O), 5.18 (2 H, s, CH_2O), 6.99 (2 H, d, *J* 7.8, ArH), 7.24–7.49 (13 H, m, ArH), 7.76 (1 H, s, ArH), 7.90–7.7.92 (3 H, m, ArH), 8.68 (1 H, d, *J* 8.8 Hz, ArH) and 8.90 (1 H, d, *J* 9.3 Hz, ArH); δ_C (75.4 MHz; $CDCl_3$) 45.8, 58.0, 66.1, 69.8, 70.2, 106.9, 107.4, 114.2, 114.8, 119.3, 123.3, 124.7, 125.6, 125.8, 127.5, 127.7, 127.9, 128.1, 128.5, 128.6, 129.8, 131.0, 131.1, 131.3, 132.7, 133.3, 133.7, 136.4, 136.5, 142.6, 156.3, 157.3, 163.0 and 196.4; EIMS (*m*/*z*) 638 $[M + H]^+$.

(3,9-Dibenzyloxybenzo[*b*]naphtho[1,2-*d*]thien-5-yl)(4-[1-methylpiperidine-4-yloxy]phenyl)methanone 8c. The procedure described above for **8b** was used for the synthesis of **8c**. From **7a** (0.1 g, 0.18 mmol), 1-methylpiperidine-4-ol (0.41 g, 3.5 mmol) and NaH (0.08 g, 3.5 mmol), **8c** (0.088 g, 76%) was obtained as a yellow oil. ν_{max} (KBr)/cm^{-1} 1597 and 2925; δ_H (300 MHz, $CDCl_3$) 1.84–1.99 (2 H, m, CH_2), 2.00–2.15 (2 H, m, CH_2), 2.26–2.40 (5 H, m, CH_2 and CH_3), 2.64–2.79 (2 H, m, CH_2), 4.42–4.54 (1 H, m, CH), 5.08 (2 H, s, CH_2O), 5.20 (2 H, s, CH_2O), 6.95 (2 H, d, *J* 7.8, ArH), 7.26–7.52 (13 H, m, ArH), 7.77 (1 H, s, ArH), 7.88–7.93 (3 H, m, ArH), 8.70 (1 H, d, *J* 8.3, ArH) and 8.91 (1 H, d, *J* 8.8, ArH); δ_C (75.4 MHz; $CDCl_3$) 14.11, 20.99, 29.60, 30.39, 45.95, 52.19, 60.31, 69.80, 70.16, 106.91, 107.39, 114.79, 115.10, 119.26, 123.34, 124.71, 125.61, 125.78, 127.46, 127.68, 127.93, 128.08, 128.45, 128.58, 129.76, 130.89, 131.03, 131.30, 132.81, 133.23, 133.66, 136.38, 136.44, 142.57, 156.25, 157.24, 161.75 and 196.34; EIMS (*m*/*z*) 664 $[M + H]^+$.

(3,9-Dibenzyloxybenzo[*b*]naphtho[1,2-*d*]thien-5-yl)(4-[2-(piperidine-1-yl)ethylamino]phenyl)methanone 8d. To a solution of 2-(piperidine-1-yl)ethylamine (0.451 g, 3.52 mmol) in DMF (5 cm^3) was added K_2CO_3 (0.486 g, 3.5 mmol) and the mixture was stirred at RT for 15 min. Then **7a** (0.1 g, 0.18 mmol) was added and the stirring was continued for 6 h at 100 °C. To the solution was added water, and the aqueous layer was extracted with AcOEt, washed with brine, dried ($MgSO_4$) and evaporated. The residue was purified by flash column chromatography using AcOEt as an eluent to give **8d** (0.101 g, 85%) as a yellow oil. ν_{max} (KBr)/cm^{-1} 1591, 2925 and 3356; δ_H (300 MHz, $CDCl_3$) 1.40–1.55 (2 H, m, CH_2), 1.56–1.64 (4 H, m, $2CH_2$), 2.32–2.49 (4 H, m, $2CH_2N$), 2.56–2.58 (2 H, m, CH_2N), 3.19–3.20 (2 H, m, CH_2N), 5.07 (2 H, s, CH_2O), 5.15 (2 H, s, CH_2O), 5.21 (1 H, s, NH), 6.57 (2 H, d, *J* 8.8, ArH), 7.23–7.49 (13 H, m, ArH), 7.74 (1 H, d, *J* 2.5, ArH), 7.83 (2 H, d, *J* 8.8, ArH), 8.02 (1 H, s, ArH), 8.67 (1 H, d, *J* 8.8, ArH), and 8.89 (1 H, d, *J* 9.8, ArH); δ_C (75.4 MHz; $CDCl_3$) 24.21, 25.77, 39.27, 54.03, 56.61, 69.75, 70.11, 106.93, 107.52, 111.34, 114.60, 119.10, 122.26, 124.58, 125.56, 126.49, 127.43, 127.67, 127.83, 127.99, 128.38, 128.52, 129.89, 130.57, 131.06, 133.07, 133.46, 134.91, 136.42, 136.49, 142.28, 152.73, 156.01, 157.03 and 195.75; EIMS (*m*/*z*) 677 $[M + H]^+$.

(3,9-Dibenzyloxybenzo[*b*]naphtho[1,2-*d*]thien-5-yl)(4-[4-isopropylpiperazin-1-yl]phenyl)methanone 8e. The procedure described above for **8d** was used for the synthesis of **8e**. From **7a** (0.1 g, 0.18 mmol), 4-isopropylpiperazine (0.451 g, 3.52 mmol) and K_2CO_3 (0.486 g, 3.5 mmol), **8e** (0.1 g, 85%) was obtained as a yellow oil. ν_{max} (KBr)/cm^{-1} 1591, 2912 and 3443; δ_H (300 MHz, $CDCl_3$) 1.09 (6 H, d, *J* 6.4, $2CH_3$), 2.63–2.66 (5 H, m, $2CH_2N$ and CH), 3.37–3.39 (4 H, m, $2CH_2N$), 5.06 (2 H, s, CH_2O), 5.14 (2 H, s, CH_2O), 6.84 (2 H, d, *J* 8.8, ArH), 7.24 (1 H, dd, *J* 2.4, 9.3, ArH), 7.37–7.49 (12 H, m, ArH), 7.77 (1 H, d, *J* 2.9, ArH), 7.86 (2 H, d, *J* 8.8, ArH), 7.91 (1 H, s, ArH), 8.67 (1 H, d, *J* 9.3, ArH) and 8.89 (1 H, d, *J* 9.8, ArH); δ_C (75.4 MHz; $CDCl_3$) 18.39, 47.20, 48.22, 54.36, 69.77, 70.13, 106.91, 107.46, 112.89, 114.66, 119.17, 122.68, 124.62, 125.59, 125.65, 127.44, 127.62, 127.69, 127.86, 128.02, 128.39, 128.54, 129.84, 130.81, 131.07, 132.62, 133.37, 134.43, 136.40, 136.48, 142.39, 154.23, 156.11, 157.09 and 195.86; EIMS (*m*/*z*) 677 $[M + H]^+$.

(3,9-Dihydroxybenzo[*b*]naphtho[1,2-*d*]furan-5-yl)(4-[2-(piperidin-1-yl)ethoxy]phenyl)methanone 8f. The procedure described above for **8b** was used for the synthesis of **8f**. From 2-(piperidin-1-yl)ethanol (0.47 g, 3.6 mmol), NaH (0.09 g, 3.6 mmol) and **7b** (0.1 g, 0.18 mmol), **8f** (0.114 g, 96%) was obtained as a yellow oil. ν_{max} (KBr)/cm^{-1} 1590 and 3020; δ_H (300 MHz, $CDCl_3$) 1.40–1.50 (2 H, m, CH_2), 1.58–1.61 (4 H, m, CH_2), 2.45–2.64 (4 H, m, CH_2), 2.78–2.89 (2 H, m, CH_2N), 4.15–4.27 (2 H, m, CH_2O), 5.08 (2 H, s, CH_2O), 5.18 (2 H, s, CH_2O), 6.97 (2 H, d, *J* 7.3, ArH), 7.17 (1 H, m, ArH), 7.25 (1 H, m, ArH), 7.35–7.52 (11 H, m, ArH), 7.79–7.80 (2 H, m, ArH), 7.90 (2 H, d, *J* 7.3, ArH), 8.24 (1 H, d, *J* 7.83, ArH) and 8.53 (1 H, d, *J* 8.28, ArH); δ_C (75.4 MHz; $CDCl_3$) 24.01, 25.78, 54.96, 57.58, 66.15, 69.82, 70.35, 97.49, 107.06, 112.61, 114.18, 114.70, 117.55, 119.90, 120.38, 122.56, 124.05, 124.99, 127.46, 127.66, 127.90, 128.05, 128.43, 128.57, 129.58, 131.07, 132.75, 133.53, 136.36, 136.50, 151.05, 156.27, 157.95, 158.66, 162.92 and 196.17; EIMS (*m*/*z*) 662 $[M + H]^+$.

(3,9-Dibenzyloxybenzo[*b*]naphtho[1,2-*d*]furan-5-yl)(4-[2-(*N*,*N*-dimethyl)ethoxy]phenyl)methanone 8g. The same procedure described above for **8b** was used for the synthesis of **8g**. From

7b (0.1 g, 0.18 mmol), 2-(dimethylamino)ethanol (0.32 g, 3.6 mmol) and NaH (0.09 g, 3.6 mmol), **8g** (0.104 g, 93%) was obtained as a yellow oil. ν_{max} (KBr)/cm^{-1} 1594 and 2931; δ_H (300 MHz, $CDCl_3$) 2.37 (6 H, s, $2CH_3$), 2.73–2.86 (2 H, m, CH_2N), 4.12–4.21 (2 H, m, CH_2), 5.08 (2 H, s, CH_2O), 5.16 (2 H, s, CH_2O), 6.99 (2 H, d, *J* 7.8, ArH), 7.14–7.17 (1 H, m, ArH), 7.23 (1 H, s, ArH), 7.36–7.51 (11 H, m, ArH), 7.80–7.82 (2 H, m, ArH), 7.91 (2 H, d, *J* 7.3, ArH), 8.23 (1 H, d, *J* 7.80, ArH) and 8.51 (1 H, d, *J* 8.31, ArH); δ_C (75.4 MHz; $CDCl_3$) 45.78, 57.93, 66.10, 69.79, 70.31, 97.45, 107.05, 112.59, 114.15, 114.73, 117.51, 119.87, 120.38, 122.54, 124.03, 124.97, 127.44, 127.65, 127.88, 128.03, 128.42, 128.55, 129.57, 131.12, 132.72, 133.47, 136.34, 136.49, 151.01, 156.25, 157.92, 158.64, 162.89 and 196.13; EIMS (*m*/*z*) 621 [M + H]$^+$.

(3,9-Dibenzyloxybenzo[*b*]naphtho[1,2-*d*]furan-5-yl)(4-[1-methylpiperidine-4-yloxy]phenyl)methanone 8h. The procedure described above for **8b** was used for the synthesis of **8h**. From **7b** (0.1 g, 0.18 mmol), 1-methylpiperidine-4-ol (0.42 g, 3.6 mmol) and NaH (0.09 g, 3.6 mmol), **8h** (0.1 g, 85%) was obtained as a yellow oil. ν_{max} (KBr)/cm^{-1} 1594 and 2931; δ_H (300 MHz, $CDCl_3$) 1.82–2.00 (2 H, m, CH_2), 2.01–2.16 (2 H, m, CH_2), 2.28–2.46 (5 H, m, CH_3 and CH_2N), 2.67–2.79 (2 H, m, CH_2N), 4.42–4.52 (1 H, m, CH), 5.08 (2 H, s, CH_2O), 5.17 (2 H, s, CH_2O), 6.95 (2 H, d, *J* 7.8, ArH), 7.15–7.16 (1 H, m, ArH), 7.24 (1 H, s, ArH), 7.35–7.51 (11 H, m, ArH), 7.80–7.82 (2 H, m, ArH), 7.90 (2 H, d, *J* 7.8, ArH), 8.24 (1 H, d, *J* 8.28, ArH) and 8.52 (1 H, d, *J* 8.28, ArH); δ_C (75.4 MHz; $CDCl_3$) 30.43, 45.99, 52.27, 69.81, 70.34, 97.48, 107.07, 112.61, 114.72, 115.08, 117.54, 119.87, 120.39, 122.57, 124.06, 124.99, 127.46, 127.67, 127.91, 128.06, 128.44, 128.57, 129.58, 130.93, 132.84, 133.49, 136.35, 136.50, 151.04, 156.27, 157.94, 158.66, 161.70 and 196.10; EIMS (*m*/*z*) 648 [M + H]$^+$.

(3,9-Dibenzyloxybenzo[*b*]naphtho[1,2-*d*]furan-5-yl)(4-[2-(piperidine-1-yl)ethylamino]phenyl)methanone 8i. The procedure described above for **8d** was used for the synthesis of **8i**. From **7b** (0.1 g, 0.18 mmol), 2-(piperidine-1-yl)ethylamine (0.463 g, 3.62 mmol) and K_2CO_3 (0.5 g, 3.62 mmol), **8i** (0.101 g, 85%) was obtained as a yellow oil. ν_{max} (KBr)/cm^{-1} 1591, 2925 and 3356; δ_H (300 MHz, $CDCl_3$) 1.45–1.48 (2 H, m, CH_2), 1.58–1.62 (4 H, m, CH_2), 2.38–2.50 (4 H, m, CH_2), 2.58–2.62 (2 H, m, CH_2N), 3.20–3.26 (2 H, m, CH_2N), 5.08 (2 H, s, CH_2O), 5.19 (3 H, m, CH_2O and NH), 6.59 (2 H, d, *J* 8.8, ArH), 7.17 (1 H, dd, *J* 2.4, 8.8, ArH), 7.26–7.28 (1 H, m, ArH), 7.31–7.55 (11 H, m, ArH), 7.74 (1 H, d, *J* 2.4, ArH), 7.80–7.83 (3 H, m, ArH), 8.25 (1 H, d, *J* 8.8, ArH) and 8.53 (1 H, d, *J* 8.8, ArH); δ_C (75.4 MHz; $CDCl_3$) 24.22, 25.77, 39.28, 54.06, 56.62, 69.81, 70.34, 97.52, 107.19, 111.34, 112.42, 113.71, 117.73, 119.52, 119.76, 122.39, 124.043, 124.90, 126.51, 127.45, 127.69, 127.84, 128.01, 128.40, 128.54, 129.54, 133.14, 134.94, 136.42, 136.57, 151.33, 152.71, 156.01, 157.73, 158.43 and 195.57; EIMS (*m*/*z*) 661 [M + H]$^+$.

(3,9-Dibenzyloxybenzo[*b*]naphtho[1,2-*d*]furan-5-yl)(4-[4-isopropylpiperazin-1-yl]phenyl)methanone 8j. The procedure described above for **8d** was used for the synthesis of **8j**. From **7b** (0.1 g, 0.18 mmol), 4-isopropylpiperazine (0.463 g, 3.62 mmol) and K_2CO_3 (0.5 g, 3.62 mmol), **8j** (0.101 g, 85%) was obtained as a yellow oil. ν_{max} (KBr)/cm^{-1} 1588 and 2962; δ_H (300 MHz, $CDCl_3$) 1.10 (6 H, d, *J* 6.4, $2CH_3$), 2.66–2.78 (5 H, m, $2CH_2$ and CH), 3.40–3.43 (4 H, m, $2CH_2$), 5.08 (2 H, s, CH_2O), 5.19 (2 H, s, CH_2O), 6.88 (2 H, d, *J* 9.3, ArH), 7.17 (1 H, dd, *J* 2.5, 8.8, ArH), 7.27 (1 H, d, *J* 2.0, ArH), 7.37–7.50 (11 H, m, ArH), 7.77 (1 H, d, *J* 2.4, ArH), 7.80 (1 H, s, ArH), 7.84 (2 H, d, *J* 8.8, ArH), 8.26 (1 H, d, *J* 8.8, ArH) and 8.53 (1 H, d, *J* 9.3, ArH); δ_C (75.4 MHz; $CDCl_3$) 18.41, 47.29, 48.27, 54.39, 69.85, 70.37, 97.57, 107.24, 112.50, 112.92, 114.08, 117.70, 119.82, 122.46, 124.07, 124.92, 127.45, 127.69, 127.86, 128.02, 128.41, 128.55, 129.59, 132.67, 134.46, 136.43, 136.58, 151.26, 154.26, 156.13, 157.83, 158.53 and 195.66; EIMS (*m*/*z*) 661 [M + H]$^+$.

(3,9-Dihydroxybenzo[*b*]naphtho[1,2-*d*]thien-5-yl)(4-[2-(piperidine-1-yl)ethoxy]phenyl)methanone 9a. To a solution of **8a**[17] (0.096 g, 0.142 mmol) in EtOH–AcOEt–H_2O 7 : 3 : 1 (10 cm^3) was added ammonium formate (0.29 g, 4.26 mmol) and black palladium (0.015 g, 0.142 mmol) and the mixture was stirred at reflux for 3 h. The black palladium was eliminated by filtration and the solvent was evaporated. The residue was purified by flash column chromatography using DCM–MeOH 9 : 1 as an eluent to give **9a** (0.064 g, 90%) as a yellow oil; δ_H (300 MHz, MeOD) 1.43–1.47 (2 H, m, CH_2), 1.64–1.68 (4 H, m, $2CH_2$), 3.00–3.06 (4 H, m, $2CH_2N$), 3.20–3.25 (2 H, m, CH_2N), 4.09–4.12 (2 H, m, CH_2O), 6.77 (2 H, d, *J* 9.2, ArH), 7.02 (1 H, dd, *J* 2.4, 8.6, ArH), 7.22–7.26 (2 H, m, ArH), 7.32 (1 H, d, *J* 2.4, ArH), 7.62 (1 H, s, ArH), 7.65 (2 H, d, *J* 8.6, ArH), 8.42 (2 H, m, 2OH), 8.55 (1 H, d, *J* 9.2, ArH) and 8.79 (1 H, d, *J* 9.2, ArH); EIMS (*m*/*z*) 498 [M + H]$^+$. To **9a** was added a solution of HCl saturated ether and the solution was stirred overnight to give the hydrochloride compound as a solid which was isolated by filtration, mp 217–218 °C; ν_{max} (KBr)/cm^{-1} 1600, 2680 and 3200; δ_H (300 MHz, DMSO) 1.67–1.79 (6 H, m, CH_2–piperidine), 2.98–3.01 (2 H, m, CH_2–piperidine), 3.45–3.58 (4 H, m, CH_2–piperidine, CH_2N), 4.45–5.52 (2 H, m, CH_2O), 7.11–7.16 (3 H, m, ArH), 7.27 (1 H, d, *J* 2.5, ArH), 7.33 (1 H, dd, *J* 2.5, 9.2, ArH), 7.48 (1 H, dd, *J* 1.8, ArH), 7.81–8.03 (2 H, m, ArH), 8.03 (1 H, s, ArH), 8.77 (1 H, d, *J* 9.2, ArH), 8.95 (1 H, d, *J* 9.2, ArH), 9.94 (1 H, s, OH), 10.05 (1 H, s, NH) and 10.16 (1 H, s, OH); δ_C (75.4 MHz; DMSO) 20.6, 21.9, 52.2, 54.1, 62.1, 108.0, 108.3, 114.4, 114.6, 118.7, 121.8, 123.2, 127.3, 130.2, 130.2, 130.6, 131.1, 131.9, 132.6, 141.6, 154.6, 155.9, 161.3 and 195.3; EIMS (*m*/*z*) 498 [M + H]$^+$; HPLC > 94.38%.

(3,9-Dihydroxybenzo[*b*]naphtho[1,2-*d*]thien-5-yl)(4-[2-(*N*,*N*-dimethyl)ethoxy]phenyl)methanone 9b. The procedure described above was used for the synthesis of **9b**. From **8b** (0.086 g, 0.135 mmol), ammonium formate (0.255 g, 4.05 mmol) and black palladium (0.014 g, 0.135 mmol) in EtOH (20 cm^3), **9b** (0.036 g, 59%) was obtained as a yellow oil. δ_H (300 MHz, MeOD) 2.88 (6 H, s, $2CH_3$), 3.45–3.55 (2 H, m, CH_2N), 4.27–4.36 (2 H, m, CH_2O), 6.96–6.99 (2 H, d, *J* 9.2, ArH), 7.09 (1 H, dd, *J* 2.4, 8.6, ArH), 7.29–7.33 (2 H, m, ArH), 7.38 (1 H, d, *J* 2.5, ArH), 7.75–7.79 (3 H, m, ArH), 8.44 (2 H, m, 2OH), 8.64 (1 H, d, *J* 9.2, ArH) and 8.87 (1 H, d, *J* 9.8 Hz, ArH); δ_C (75.4 MHz; MeOD) 44.03, 57.48, 63.79, 109.28, 110.35, 115.52, 115.84, 119.83, 123.98, 125.90, 126.26, 127.18, 129.91, 132.57, 132.83, 133.00, 133.43, 133.84, 134.45, 144.14, 156.39, 157.70, 163.39 and 198.46. To **9b** was added a solution of HCl saturated ether and the solution was stirred overnight to

give the hydrochloride compound as a solid which was isolated by filtration, mp 188–189 °C; ν_{max} (KBr)/cm^{-1} 1600, 2710 and 3220; δ_H (300 MHz, DMSO) 2.84 (6 H, s, 2CH$_3$), 3.30–3.49 (2 H, m, CH$_2$N), 4.41–4.43 (2 H, m, CH$_2$O), 7.12–7.15 (3 H, m, ArH), 7.24–7.25 (1 H, m, ArH), 7.30–7.35 (1 H, m, ArH), 7.46–7.49 (1 H, m, ArH), 7.81 (2 H, m, ArH), 8.02 (1 H, s, ArH), 7.72–7.80 (1 H, m, ArH), 8.92–8.98 (1 H, m, ArH), 9.70 (1 H, s, NH), 9.92 (1 H, s, OH) and 10.13 (1 H, s, OH); EIMS (*m*/*z*) 458 [M + H]$^+$; HPLC purity: 91.27%.

(3,9-Dihydroxybenzo[*b*]naphtho[1,2-*d*]thien-5-yl)(4-[1-methylpiperidine-4-yloxy]phenyl)methanone 9c. The procedure described above was used for the synthesis of **9c**. From **8c** (0.088 g, 0.133 mmol), ammonium formate (0.251 g, 3.99 mmol) and black palladium (0.014 g, 0.133 mmol) in EtOH–AcOEt–H$_2$O 7 : 3 : 1 (20 cm^3), **9c** (0.048 g, 75%) was obtained as a yellow oil. δ_H (300 MHz, MeOD) 1.90–2.08 (2 H, m, CH$_2$), 2.09–2.18 (2 H, m, CH$_2$), 2.72 (3 H, s, CH$_3$), 3.02–3.15 (2 H, m, CH$_2$N), 3.16–3.27 (2 H, m, CH$_2$N), 4.60–4.69 (1 H, m, CH), 6.95 (2 H, d, *J* 7.8, ArH), 7.09–7.11 (1 H, m, ArH), 7.29–7.39 (3 H, m, ArH), 7.39 (1 H, s, ArH), 7.74–7.77 (3 H, m, ArH), 8.53 (2 H, m, 2OH), 8.65 (1 H, d, *J* 9.2, ArH) and 8.88 (1 H, d, *J* 8.6, ArH). To **9c** was added a solution of HCl saturated ether and the solution was stirred overnight to give the hydrochloride compound as a solid which was isolated by filtration, mp 187–188 °C; ν_{max} (KBr)/cm^{-1} 1600, 2715 and 3230; δ_H (300 MHz, DMSO) 1.87–2.28 (4 H, m, 2CH$_2$–piperidine), 2.76 (3 H, s, CH$_3$), 3.00–3.40 (4 H, m, 2 × CH$_2$–piperidine), 4.90 (1 H, m, CH–piperidine), 7.11–7.18 (3 H, m, ArH), 7.28 (1 H, s, ArH), 7.33 (1 H, dd, *J* 2.4, 9.2, ArH), 7.48 (1 H, d, *J* 2.4, ArH), 7.78–7.82 (2 H, m, ArH), 8.04 (1 H, s, ArH), 8.76 (1 H, d, *J* 9.2, ArH), 8.95 (1 H, d, *J* 9.2, ArH), 9.94 (1 H, s, OH), 10.06 (1 H, s, OH) and 10.42 (1 H, s, NH); δ_C (75.4 MHz; MeOD) 41.47, 41.83, 47.99, 51.14, 65.99, 69.96, 107.98, 108.00, 108.31, 113.70, 114.56, 114.56, 114.93, 115.33, 118.66, 121.67, 123.19, 127.28, 130.16, 130.25, 131.07, 131.97, 132.65, 132.67, 141.61, 154.57, 155.89, 160.45, 160.68 and 195.15; HPLC purity: 94.38%.

(3,9-Dihydroxybenzo[*b*]naphtho[1,2-*d*]thien-5-yl)(4-[2-(piperidine-1-yl)ethylamino]phenyl)methanone 9d. The procedure described above was used for the synthesis of **9d**. From **8d** (0.093 g, 0.137 mmol), ammonium formate (0.258 g, 4.12 mmol) and black palladium (0.015 g, 0.137 mmol) in MeOH (20 cm^3), **9d** (0.060 g, 90%) was obtained as a yellow oil. δ_H (300 MHz, MeOD) 1.48–1.50 (2 H, m, CH$_2$), 1.65–1.69 (4 H, m, 2CH$_2$), 2.83–2.90 (6 H, m, 3CH$_2$N), 3.34–3.41 (2 H, m, CH$_2$N), 6.56 (2 H, d, *J* 8.6, ArH), 7.10 (1 H, dd, *J* 2.4, 9.2, ArH), 7.28–7.34 (3 H, m, ArH), 7.64 (2 H, d, *J* 9.2, ArH), 7.69 (1 H, s, ArH), 8.65 (1 H, d, *J* 9.2, ArH) and 8.88 (1 H, d, *J* 9.8, ArH); δ_C (75.4 MHz; MeOD) 22.81, 24.26, 38.56, 54.55, 56.51, 109.36, 110.48, 112.63, 115.80, 119.80, 122.83, 125.87, 126.17, 126.18, 126.99, 127.78, 130.03, 132.13, 132.57, 133.64, 134.34, 135.63, 143.85, 154.18, 156.14, 157.50 and 198.28.

(3,9-Dihydroxybenzo[*b*]naphtho[1,2-*d*]thien-5-yl)(4-[4-isopropylpiperazin-1-yl]phenyl)methanone 9e. The procedure described above was used for the synthesis of **9e**. From **8e** (0.095 g, 0.14 mmol), ammonium formate (0.265 g, 4.21 mmol) and black palladium (0.015 g, 0.140 mmol), **9e** (0.069 g, 99%) was obtained as a yellow oil. δ_H (300 MHz, MeOD) 1.02 (6 H, d, *J* 6.7, 2CH$_3$), 2.52–2.53 (5 H, m, 2CH$_2$, CH), 3.23–3.25 (4 H, m, 2CH$_2$N), 6.76 (2 H, d, *J* 9.2, ArH), 7.11 (1 H, dd, *J* 2.4, 8.6, ArH), 7.28–7.34 (3 H, m, ArH), 7.67 (2 H, d, *J* 8.6, ArH), 7.74 (1 H, s, ArH), 8.68 (1 H, d, *J* 8.6, ArH) and 8.90 (1 H, d, *J* 9.2, ArH); δ_C (75.4 MHz; MeOD) 18.09, 47.08, 49.24, 56.99, 109.35, 110.47, 114.45, 115.81, 119.82, 123.28, 125.92, 126.15, 126.20, 127.08, 129.04, 130.06, 132.39, 132.62, 133.63, 133.79, 135.31, 144.00, 155.48, 156.22, 157.58 and 198.35. To **9e** was added a solution of HCl saturated ether and the solution was stirred overnight to give the hydrochloride compound as a solid which was isolated by filtration; ν_{max} (KBr)/cm^{-1} 1595, 2920 and 3185; δ_H (300 MHz, DMSO) 1.29 (6 H, d, *J* 6.6, 2 × CH$_3$), 3.10–3.35 (4 H, m, 2CH$_2$N), 3.49–3.53 (3 H, m, CH$_2$N, CH), 4.10–4.14 (2 H, m, CH$_2$N), 7.08–7.14 (3 H, m, ArH), 7.24 (1 H, d, *J* 2.5, ArH), 7.32 (1 H, dd, *J* 2.6, 9.1, ArH), 7.47 (1 H, d, *J* 2.5, ArH), 7.71 (2 H, d, *J* 8.9, ArH), 7.98 (1 H, s, ArH), 8.75 (1 H, d, *J* 9.2, ArH), 8.93 (1 H, d, *J* 9.2, ArH), 9.84 (1 H, s, OH), 10.06 (1 H, s, OH) and 10.11 (2 H, m, 2NH). HPLC purity: 92.49%.

(3,9-Dihydroxybenzo[*b*]naphtho[1,2-*d*]furan-5-yl)(4-[2-(piperidine-1-yl)ethoxy]phenyl)methanone 9f. The procedure described above was used for the synthesis of **9f**. From **8f** (0.113 g, 0.170 mmol), ammonium formate (0.321 g, 5.1 mmol) and black palladium (0.018 g, 0.170 mmol), **9f** (0.100 g, 85%) was obtained as a yellow oil. δ_H (300 MHz, MeOD) 1.15–1.26 (2 H, m, CH$_2$), 1.30–1.44 (4 H, m, CH$_2$), 2.45–2.61 (4 H, m, CH$_2$), 2.70–2.80 (2 H, m, CH$_2$N), 3.75–3.89 (2 H, m, CH$_2$O), 6.55 (2 H, d, *J* 7.9, ArH), 6.64–6.71 (2 H, m, ArH), 6.98–7.01 (1 H, m, ArH), 7.14–7.16 (1 H, m, ArH), 7.26–7.28 (1 H, m, ArH), 7.41 (2 H, d, *J* 7.3, ArH), 7.85 (1 H, d, *J* 7.95, ArH), 8.15 (1 H, d, *J* 9.15, ArH) and 8.26 (2 H, m, 2OH); δ_C (75.4 MHz; MeOD) 23.63, 25.07, 55.17, 57.61, 64.78, 99.33, 110.10, 113.71, 115.32, 117.47, 120.35, 121.88, 123.89, 124.29, 126.46, 131.16, 132.59, 133.81, 134.02, 151.59, 156.24, 159.17, 159.65, 163.71 and 198.05. To **9f** was added a solution of HCl saturated ether and the solution was stirred overnight to give the hydrochloride compound as a solid which was isolated by filtration, mp 267–268 °C; ν_{max} (KBr)/cm^{-1} 1620, 2720 and 3180; δ_H (300 MHz, DMSO) 1.67–1.80 (6 H, m, CH$_2$–piperidine), 2.92–3.10 (2 H, m, CH$_2$–piperidine), 3.45–3.59 (4 H, m, CH$_2$–piperidine, CH$_2$N), 4.50–4.58 (2 H, m, CH$_2$O), 7.02 (1 H, dd, *J* 1.9, 8.6, ArH), 7.12–7.15 (3 H, m, ArH), 7.33–7.37 (2 H, m, ArH), 7.81–7.84 (3 H, m, ArH), 8.39 (1 H, d, *J* 8.8, ArH), 8.63 (1 H, d, *J* 8.8, ArH), 9.86 (1 H, s, NH), 10.19 (1 H, s, OH) and 10.70 (1 H, s, OH); δ_C (75.4 MHz; MeOD) 21.50, 22.30, 52.57, 54.50, 62.69, 98.26, 108.47, 112.86, 113.32, 114.72, 115.34, 119.61, 119.72, 122.03, 122.92, 125.45, 129.26, 131.02, 132.35, 132.81, 149.74, 154.94, 157.57, 157.89, 161.70 and 195.29; EIMS (*m*/*z*) 482 [M + H]$^+$. HPLC purity: 97.59%.

(3,9-Dihydroxybenzo[*b*]naphtho[1,2-*d*]furan-5-yl)(4-[2-(*N*,*N*-dimethyl)ethoxy]phenyl)methanone 9g. The procedure described above was used for the synthesis of **9g**. From **8g** (0.101 g, 0.161 mmol), ammonium formate (0.304 g, 4.83 mmol) and black palladium, **9g** (0.067 g, 95%) was obtained as a yellow oil. δ_H (300 MHz, MeOD) 2.88 (6 H, s, 2CH$_3$), 3.42–3.55 (2 H, m, CH$_2$N), 4.33–4.44 (2 H, m, CH$_2$O),

6.97–7.03 (4 H, m, ArH), 7.30–7.33 (1 H, m, ArH), 7.43–7.45 (1 H, m, ArH), 7.66 (1 H, s, ArH), 7.81–7.84 (2 H, m, ArH), 8.23 (1 H, d, *J* 9.15, ArH), 8.51 (2 H, m, 2OH) and 8.53 (1 H, d, *J* 9.15, ArH). To **9g** was added a solution of HCl saturated ether and the solution was stirred overnight to give the hydrochloride compound as a solid which was isolated by filtration, mp 136–138 °C; ν_{max} (KBr)/cm^{-1} 1623, 2700 and 3370; δ_H (300 MHz, DMSO) 2.84 (6 H, s, 2CH_3), 3.49–3.56 (2 H, m, CH_2), 4.41–4.52 (2 H, m, CH_2), 7.00–7.02 (1 H, m, ArH), 7.10–7.20 (3 H, m, ArH), 7.32–7.35 (2 H, m, ArH), 7.81–7.84 (3 H, m, ArH), 8.39 (1 H, d, *J* 8.6, ArH), 8.63 (1 H, d, *J* 8.6, ArH), 9.89 (1 H, s, OH), 10.22 (1 H, s, OH) and 10.34 (1 H, s, NH); δ_C (75.4 MHz; MeOD) 42.75, 55.09, 62.71, 98.32, 108.52, 112.95, 113.41, 114.83, 115.40, 119.70, 119.78, 122.09, 123.03, 125.56, 129.32, 131.10, 132.42, 132.87, 149.81, 155.00, 157.63, 157.96, 161.77 and 195.41; EIMS (*m*/*z*) 515 [M + H]$^+$.

(3,9-Dihydroxybenzo[*b*]naphtho[1,2-*d*]furan-5-yl)(4-[1-methylpiperidine-4-yloxy]phenyl)methanone 9h. The procedure described above was used for the synthesis of **9h**. From **8h** (0.105 g, 0.162 mmol), ammonium formate (0.306 g, 4.86 mmol) and black palladium (0.017 g, 0.162 mmol), **9h** (0.053 g, 71%) was obtained as a yellow oil. δ_H (300 MHz, MeOD) 1.85–1.90 (2 H, m, CH_2), 1.89–2.10 (2 H, m, CH_2), 2.29 (3 H, s, CH_3), 2.32–2.49 (2 H, m, CH_2N), 2.64–2.76 (2 H, m, CH_2N), 4.50–4.62 (1 H, m, CH), 6.99–7.06 (4 H, m, ArH), 7.31–7.34 (1 H, m, ArH), 7.40–7.42 (1 H, m, ArH), 7.70 (1 H, s, ArH), 7.82 (2 H, d, *J* 8.0, ArH), 8.65 (1 H, d, *J* 7.9, ArH) and 8.88 (1 H, d, *J* 8.5, ArH). To **9h** was added a solution of HCl saturated ether and the solution was stirred overnight to give the hydrochloride compound as a solid which was isolated by filtration, mp 269–270 °C; ν_{max} (KBr)/cm^{-1} 1625, 2740 and 3160; δ_H (300 MHz, DMSO) 1.95–2.05 (2 H, m, CH_2), 2.10–2.25 (2 H, m, CH_2), 2.73 (3 H, s, CH_3), 3.10–3.50 (4 H, m, 2CH_2), 4.78–4.82 (1 H, m, CH), 6.99–7.06 (1 H, m, ArH), 7.11–7.20 (3 H, m, ArH), 7.30–7.40 (2 H, m, ArH), 7.75–7.90 (3 H, m, ArH), 8.38 (1 H, d, *J* 7.9, ArH), 8.62 (1 H, d, *J* 8.5, ArH), 9.91 (1 H, s, OH) and 10.23–10.25 (2 H, m, OH, NH); δ_C (75.4 MHz; DMSO) 30.08, 45.42, 52.01, 98.33, 108.48, 112.87, 113.26, 115.46, 119.59, 119.66, 122.08, 123.03, 125.56, 129.30, 130.17, 130.20, 132.53, 133.08, 149.86, 154.94, 157.60, 157.85, 161.64 and 195.26; EIMS (*m*/*z*) 468 [M + H]$^+$; HPLC purity: 98.60%.

(3,9-Dihydroxybenzo[*b*]naphtho[1,2-*d*]furan-5-yl)(4-[2-(piperidine-1-yl)ethylamino]phenyl)methanone 9i. The procedure described above was used for the synthesis of **9i**. From **8i** (0.086 g, 0.130 mmol), ammonium formate (0.049 g, 0.78 mmol) and black palladium (0.014 g, 0.130 mmol), **9i** (0.054 g, 87%) was obtained as a yellow oil. δ_H (300 MHz, MeOD) 1.39–1.41 (2 H, m, CH_2), 1.54–1.57 (4 H, m, 2CH_2), 2.56–2.64 (6 H, m, 3CH_2N), 3.22–3.27 (2 H, m, CH_2N), 6.49 (2 H, d, *J* 8.6, ArH), 6.92 (1 H, dd, *J* 1.8, 8.6, ArH), 7.00 (1 H, d, *J* 2.4, ArH), 7.25 (1 H, dd, *J* 2.4, 9.2, ArH), 7.31 (1 H, d, *J* 2.4, ArH), 7.55 (1 H, s, ArH), 7.60 (2 H, d, *J* 8.5, ArH), 8.14 (1 H, d, *J* 8.6, ArH) and 8.44 (1 H, d, *J* 9.2, ArH); δ_C (75.4 MHz; MeOD) 24.23, 25.68, 39.88, 55.14, 57.72, 99.33, 110.14, 112.34, 113.57, 114.10, 117.73, 120.28, 121.01, 123.71, 124.33, 126.38, 127.19, 131.11, 134.42, 135.64, 152.00, 154.76, 155.91, 158.91, 159.50 and 198.04. To **9i** was added a solution of HCl saturated ether and the solution was stirred overnight to give the hydrochloride compound as a solid which was isolated by filtration, mp 235–236 °C; δ_H (300 MHz, DMSO) 1.67–1.76 (6 H, m, 3CH_2), 2.70–3.00 (2 H, m, CH_2), 3.12–3.25 (2 H, m, CH_2), 3.55–3.60 (4 H, m, 2CH_2), 6.70 (2 H, d, *J* 8.5, ArH), 7.00 (1 H, dd, *J* 8.5, ArH), 7.14 (1 H, m, ArH), 7.24 (1 H, m, ArH), 7.31 (1 H, dd, *J* 8.5, ArH), 7.62 (2 H, d, *J* 8.5, ArH), 7.24 (1 H, s, ArH), 8.36 (1 H, d, *J* 8.5, ArH), 8.59 (1 H, d, *J* 9.2, ArH), 9.81 (1 H, s, OH) and 10.10–10.12 (3 H, m, OH, 2 × NH); δ_C (75.4 MHz; DMSO) 21.35, 22.55, 36.92, 52.42, 54.26, 98.43, 108.74, 111.54, 112.36, 112.90, 115.69, 118.96, 119.68, 122.17, 122.98, 125.56, 125.84, 129.39, 132.67, 134.47, 150.14, 152.73, 154.75, 157.52, 157.74 and 194.52; EIMS (*m*/*z*) 481 [M + H]$^+$; HPLC purity: 93.23%.

(3,9-Dihydroxybenzo[*b*]naphtho[1,2-*d*]furan-5-yl)(4-[4-isopropylpiperazin-1-yl]phenyl)methanone 9j. The procedure described above was used for the synthesis of **9j**. From **8j** (0.101 g, 0.153 mmol), ammonium formate (0.057 g, 0.918 mmol) and black palladium (0.016 g, 0.153 mmol) in MeOH–AcOEt 1 : 1 (10 cm^3), **9j** (0.058 g, 79%) was obtained as a yellow oil. δ_H (300 MHz, MeOD) 0.96 (6 H, d, *J* 6.7, 2CH_3), 2.51–2.61 (5 H, m, 2CH_2N, CH), 3.15–3.29 (4 H, m, 2CH_2N), 6.71 (2 H, d, *J* 8.5, ArH), 6.96 (1 H, dd, *J* 1.8, 8.6, ArH), 7.03 (1 H, d, *J* 2.4, ArH), 7.29 (1 H, dd, *J* 1.8, 8.5, ArH), 7.37 (1 H, d, *J* 1.8, ArH), 7.59 (1 H, s, ArH), 7.62 (2 H, d, *J* 9.2, ArH), 8.18 (1 H, d, *J* 8.6, ArH) and 8.49 (1 H, d, *J* 9.2, ArH); δ_C (75.4 MHz; MeOD) 18.47, 47.54, 49.39, 56.07, 99.37, 110.18, 113.64, 114.16, 114.57, 117.70, 120.34, 121.31, 123.79, 124.34, 126.40, 128.63, 131.15, 133.81, 135.17, 151.93, 155.77, 156.01, 158.99, 159.57 and 198.05. To **9j** was added a solution of HCl saturated ether and the solution was stirred overnight to give the hydrochloride compound as a solid which was isolated by filtration, mp 251 °C; ν_{max} (KBr)/cm^{-1} 1620, 2680 and 3180; δ_H (300 MHz, DMSO) 1.30 (6 H, d, *J* 6.72, 2 × CH_3), 3.09–3.16 (2 H, m, CH_2N), 3.31–3.60 (5 H, m, 2CH_2N, CH), 4.09–4.13 (2 H, m, CH_2N), 7.01 (1 H, dd, *J* 8.5, ArH), 7.08 (2 H, d, *J* 8.5, ArH), 7.15 (1 H, d, *J* 1.8, ArH), 7.27 (1 H, s, ArH), 7.33 (1 H, dd, *J* 1.8, 9.2, ArH), 7.71 (2 H, d, *J* 8.5, ArH), 7.79 (1 H, s, ArH), 8.37 (1 H, d, *J* 9.2, ArH), 8.61 (1 H, d, *J* 9.2, ArH), 9.84 (1 H, s, OH), 10.19 (1 H, s, OH) and 10.58–10.67 (2 H, m, 2 × NH); δ_C (75.4 MHz; DMSO) 21.30, 22.49, 36.90, 52.38, 54.23, 98.39, 108.70, 111.50, 112.33, 112.85, 115.65, 118.91, 119.63, 122.13, 122.92, 125.82, 129.35, 132.61, 134.43, 150.10, 152.67, 154.70, 157.48, 157.69 and 194.46; EIMS (*m*/*z*) 481 [M + H]$^+$; HPLC purity: 94.32%.

3,9-Dihydroxybenzo[*b*]naphtho[1,2-*d*]thiophene-5-carboxylic acid 10. Nitrile **3** (60 mg, 0.206 mmol) was treated with a 6 N aqueous solution of NaOH (0.72 g in 3 cm^3) and the mixture was heated for 24 h. After cooling, HCl 6 N was added and the solid formed was isolated by filtration and purified by column chromatography on silica gel using DCM–MeOH 9 : 1 as an eluent to give **10** (62 mg, 97%) as a white solid. δ_H (300 MHz, DMSO) 7.13 (1 H, d, *J* 8.5, ArH), 7.34 (1 H, d, *J* 8.5, ArH), 7.49 (1 H, s, ArH), 8.47 (1 H, s, ArH), 8.60 (1 H, s, ArH), 8.77 (1 H, d, *J* 9.1, ArH), 8.94 (1 H, d, *J* 9.1, ArH), 10.02 (1 H, s, OH), 10.21 (1 H, s, OH), 13.11 (1 H, br s, COOH);

δ_C (75.4 MHz; DMSO) 104.5, 107.7, 108.5, 115.6, 118.4, 120.2, 122.8, 126.2, 127.2, 129.0, 129.2, 131.6, 132.1, 133.3, 143.3, 156.6 and 157.3; EIMS (*m*/*z*) 290 $[M - H]^+$.

Methyl 3,9-dihydroxybenzo[*b*]naphtho[1,2-*d*]thiophene-5-carboxylate 11. A solution of acid **10** (39 mg, 0.126 mmol) in MeOH (3 cm^3), in the presence of a catalytic amount of H_2SO_4, was heated for 24 h. After evaporation of MeOH and purification by column chromatography on silica gel using DCM–MeOH 15 : 1 as an eluent, the ester **11** was obtained (25 mg, 62%) as an oil. δ_H (300 MHz, DMSO) 3.95 (3 H, s, CH_3), 7.12 (1 H, dd, *J* 9.2 and 1.8, ArH), 7.35 (1 H, dd, *J* 9.2 and 2.4, ArH), 7.49 (1 H, d, *J* 1.8, ArH), 8.36 (1 H, d, *J* 2.4, ArH), 8.62 (1 H, s, ArH), 8.78 (1 H, d, *J* 9.2, ArH), 8.95 (1 H, d, *J* 9.2, ArH), 10.07 (1 H, br s, OH) and 10.17 (1 H, br s, OH); δ_C (75.4 MHz; DMSO) 167.2, 156.8, 155.8, 143.0, 132.8, 131.3, 131.1, 127.5, 126.6, 126.0, 125.3, 123.9, 122.7, 118.9, 115.2, 109.0 and 108.5.

Computational methods

The theoretical study of the binding mode has been carried out in both subtypes of estrogen receptor, α and β. As macromolecules, the crystallographic structures of the two receptor subtypes in complex with several ligands have been selected: ERα in complex with estradiol (PDB 1A52), raloxifene (PDB 1ERR), genistein (PDB 1X7R), WAY-244 (PDB 1X7E), and 4-hydroxytamoxifen (PDB 3ERT), and ERβ in complex with genistein (PDB 1X7J), THC (PDB 1L2J), WAY-202196 (PDB 1YYE), and 4-hydroxytamoxifen (PDB 2FSZ). Water molecules close to the amino acids Arg394 (ERβ Arg346) and Glu353 (Glu305 ERβ) have been kept for the docking procedures. Ligands were built using the Maestro LigPrep module (www.schrodinger.com). Optimization of the geometry and the charges calculation were performed by using program Gaussian 03[20] at the B3LYP/3-21G* level. Once the compounds were optimized, atom types and bond types were assigned, and mol2 files were generated. Macromolecules geometry was refined by using the Protein Preparation module in Maestro. Two different docking programs were employed in order to contrast and compare the results: AutoDock4[21] and Glide.[22,23] General protocols are described as follows.

Docking studies with AutoDock4. Docking regions were defined considering a box of 80, 80 and 90 points in the *x*, *y*, and *z* axes. The grids were built by focusing on the ER binding site. For the calculation of energy maps, a grid spacing of 0.375 Å and a distance-dependent dielectric constant were used by means of AutoGrid4. The docking was carried out using the Lamarckian genetic algorithm, leaving all the bonds as rotatable. The program searched until a maximum of 100 conformations and the procedure was repeated 100 times (runs). After docking, the 100 solutions were clustered in groups with RMSD less than 1.0 Å. For all other parameters, the default values were used with AutoDock Tools.

Docking studies with Glide. Interaction maps of the binding site were generated using the application "Receptor grid generation", included in the Glide module, positioning the center of the box on the center of the bound ligand present in the crystallographic structure. Box size was able to enclose the LBD together with helix-12, and was similar to the box defined with AutoDock. The docking procedure was performed with the XP (extra precision) mode and a van der Waals radii scale factor of 1.0/0.8 for the receptor and the ligand, respectively. Induced Fit Docking was also used, and contained constrained minimization of the receptor with an RMSD cutoff of 0.18 Å, and Prime-side-chain prediction on residues within 5 Å of any ligand pose. Glide redocking was performed in structures within 30 kcal mol^{-1} of the lowest energy structure with a van der Waals scaling of 1.0/0.8 for the receptor and the ligand, respectively.

Molecular dynamics simulations. The protein–ligand system was first minimized in vacuum for 1000 steps of steepest descent followed by 4000 steps of conjugate gradient using the Amber11 program.[24] All Cα atoms were restrained to their initial coordinates. The resulting minimized complex was solvated by a box of TIP3P waters which extended at least 8 Å away from any given protein atom. The SHAKE algorithm was applied to all hydrogen-containing bonds[25] and a 1 fs integration step was used. The simulation used periodic boundary conditions, and the electrostatic interactions were represented using the smooth particle mesh Ewald method,[26] with a grid spacing of 1 Å. Each system was gently annealed from 100 to 300 K over a period of 25 ps. The systems were then maintained at a temperature of 300 K during 50 ps with positional restraints (α-carbon atoms), together with a distance restraint to the hydrogen bond between the Asp303 carboxylate and the piperidinium NH group, and progressive energy minimizations, gradually releasing the restraints of the solute followed by a 20 ps heating phase from 100 to 300 K, whereafter restraints were removed. Finally, two production simulations were continued. The first one maintained the distance restraint between the Asp303 carboxylate and the piperidinium NH during 500 ps, plus one additional nanosecond without restriction. The second one continued the MD simulation during 2 ns with no restriction. Coordinate trajectories were recorded each 2 ps throughout all equilibration and production runs (RMSD, ESI†).

Biological assays

Chemicals. 17-β-Estradiol, neutral red, dextran coated charcoal, PSB, Tween-20, BSA, ICI 180.780, 4-hydroxytamoxifen, insulin were purchased from Sigma-Aldrich. Estradiol [2,4,6,7,16,17-3*H*(*N*)], scintillation counting liquid (Optifase HiSafe2) were obtained from Perkin-Elmer (Salem, MA). Estrogen receptors α and β produced in insect cells and sodium pyruvate were purchased from Invitrogen. Cell culture medium DMEM, EMEM, FBS, antibiotics, trypsin-EDTA, amino acids, L-glutamine were purchased from Lonza. DCC-FBS was obtained from Hyclone (Erembodegem, Aalst, Belgium).

Receptor binding studies: *in vitro* competitive binding assay. The relative binding affinity (RBA) of the compounds for the estrogen receptors was determined by a competition assay, according to the method described by Arcaro with some modifications.[19] Purified full-length human estrogen receptors α and β were incubated for 4 h at 23 °C with different concentrations of compounds in the presence of 5 nM [2,4,6,7,16,17-3*H*]-estradiol

in 150 µl of total volume. The stocks of test compounds were prepared in DMSO. All these compounds, including [2,4,6,7,16,17-3*H*]-estradiol and receptors, were diluted in Tween/PBS buffer (99.85 : 0.15 w/v). A vehicle control contained 0.1% of DMSO. After incubation, the non-bound [2,4,6,7,16,17-3*H*]-estradiol was removed by adding a mixture of 10% DCC and 2% albumin bovine serum, incubating for 15 min at 4 °C, followed by centrifugation at 6000 g for 5 min at 4 °C. 150 µl of the supernatant was added to 4 cm^3 of scintillation liquid and the radioactivity of bound estradiol was measured in a liquid scintillation counter Beckman LS 6500 (Beckman Coulter, Inc.). Three independent experiments with three repetitions for each compound were performed. Results were expressed as the percentage of specific binding of [2,4,6,7,16,17-3*H*]-estradiol to ER *versus* log of competitor concentration. Graph Pad Prism software (non-linear regression analysis) was used to calculate the concentration needed to displace 50% of [2,4,6,7,16,17-3*H*]-estradiol (IC_{50}). To compare binding affinities of the test compounds to those reported in the literature, IC_{50} values were converted to RBA values using estradiol as a standard. The values of IC_{50} for estradiol were 8.98 and 6.87 nM for ERα and ERβ, respectively. The RBA of estradiol was arbitrarily set at 100 (RBA = (IC_{50} of E_2)/IC_{50} of ligand × 100).

Estrogenic and antiestrogenic activities. MCF-7 cells were seeded in 96-well plates at 5×10^3 cells per well in DMEM containing 10% FBS, 0.01 mg cm^{-3} of insulin solution and 0.1 mM nonessential amino acids. After 24 h, the medium was changed to EMEM without phenol red, containing 5% dextran-coated charcoal stripped FBS (DCC-FBS), 0.1 mM nonessential amino acids, 1 mM sodium pyruvate and 2 mM L-glutamine, and was preincubated for 3 days prior to treatment. Afterwards, different concentrations of the test compounds (0.1–20 µM) were added to the cells with/without 1 pM estradiol, in order to test the capacity to induce or prevent the proliferation of MCF-7 cells. The final vehicle concentration of maximally 0.1% of DMSO (and 0.1% of ethanol in the case of treatment with estradiol) served as a solvent control. On day 4, the medium in the plates containing the compounds was refreshed. On day 8, cell proliferation was determined by the Neutral Red uptake assay, which provides a quantitative estimation of the number of viable cells. Briefly, the medium was removed and 200 µl of neutral red solution (50 µg cm^{-3}) was added, and incubated for 2 h. Afterwards, the cultures were carefully washed twice with PBS, and the extraction solution was added (250 µL of 1% acetic acid, 50% ethanol), and incubated for 15 min at room temperature. The absorbance was measured at 540 nm wavelength in a plate reader (Biotec). The viability was calculated considering the controls without test substance as 100% viable.

Agonist/antagonist profile. Reporter cells were dispensed in a 96-well plate and then immediately dosed with the test compounds. Following overnight incubation, the treatment media were discarded and the luciferase detection reagent was added. The intensity of light emission from the ensuing luciferase reaction provides a measure that is directly proportional to the level of ER activation in the reporter cells. The assays were configured to perform agonist and antagonist dose–response curves. In order to obtain agonist dose–response curves, ER reporter cells were treated with media alone (estradiol was used as a positive control agonist). To perform receptor inhibition studies a co-mix of a known agonist (estradiol: 150 and 111 pM corresponding to ~EC_{70} for the ERα and ERβ assay, respectively) and a dilution series of the test compounds was prepared. IC182 780 was used as an antagonist positive control. The final solvent control did not exceed 0.1% of DMSO. All measurements were performed in triplicate.

Abbreviations

BSC	basic side chain
PDB	Protein Data Bank
DCM	dichloromethane
THF	tetrahydrofuran
DMF	dimethylformamide
RT	room temperature
MD	molecular dynamics
RMSD	root-mean-square deviation
RBA	relative binding affinity

Acknowledgements

This work was supported by the Spanish Ministry of Science and Innovation (SAF2008-00945, CTQ2011-24741 and CSD2007-00063) and Fundación Universitaria San Pablo CEU (USP-PC 13/10). Grant to J. J. R. from Fundación Universitaria San Pablo CEU is also acknowledged. We thank EADS-CASA for fellowships to K. F., M. M., J. C. and S. D.

References

1 S. Nilsson and J. A. Gustafsson, *Clin. Pharmacol. Ther. (St. Louis)*, 2011, **89**, 44–55.
2 J. A. Katzenellenbogen, R. Muthyala and B. S. Katzenellenbogen, *Pure Appl. Chem.*, 2003, **75**, 2397–2403.
3 S. Nilsson, K. F. Koehler and J. A. Gustafsson, *Nat. Rev. Drug Discovery*, 2011, **10**, 778–792.
4 F. Minutolo, M. Macchia, B. S. Katzenellenbogen and J. A. Katzenellenbogen, *Med. Res. Rev.*, 2011, **31**, 364–442.
5 H. A. Harris, J. A. Katzenellenbogen and B. S. Katzenellenbogen, *Endocrinology*, 2002, **143**, 4172–4177.
6 H. A. Harris, L. M. Albert, Y. Leathurby, M. S. Malamas, R. E. Mewshaw, C. P. Miller, Y. P. Kharode, J. Marzolf, B. S. Komm, R. C. Winneker, D. E. Frail, R. A. Henderson, Y. Zhu and J. C. Keith, *Endocrinology*, 2003, **144**, 4241–4249.
7 M. J. Meyers, J. Sun, K. E. Carlson, G. A. Marriner, B. S. Katzenellenbogen and J. A. Katzenellenbogen, *J. Med. Chem.*, 2001, **44**, 4230–4251.
8 R. E. Mewshaw, J. Edsall, J. Richard, C. Yang, E. S. Manas, Z. B. Xu, R. A. Henderson, J. C. Keith Jr. and H. A. Harris, *J. Med. Chem.*, 2005, **48**, 3953–3979.
9 E. S. Manas, R. J. Unwalla, Z. B. Xu, M. S. Malamas, C. P. Miller, H. A. Harris, C. Hsiao, T. Akopian, W.-T. Hum, K. Malakian, S. Wolfrom, A. Bapat, R. A. Bhat, M. L. Stahl, W. S. Somers and J. C. Alvarez, *J. Am. Chem. Soc.*, 2004, **126**, 15106–15119.
10 M. De Angelis, F. Stossi, K. A. Carlson, B. S. Katzenellenbogen and J. A. Katzenellenbogen, *J. Med. Chem.*, 2005, **48**, 1132–1144.
11 J. Sun, M. J. Meyers, B. E. Fink, R. Rajendran, J. A. Katzenellenbogen and B. S. Katzenellenbogen, *Endocrinology*, 1999, **140**, 800–804.
12 M. J. Meyers, J. Sun, K. E. Carlson, B. S. Katzenellenbogen and J. A. Katzenellenbogen, *J. Med. Chem.*, 1999, **42**, 2456–2468.
13 A. M. Brzozowski, A. C. W. Pike, Z. Dauter, R. E. Hubbard, T. Bonn, O. Engström, L. Öhman, G. L. Greene, J. A. Gustafsson and M. Carlquist, *Nature*, 1997, **389**, 753–758.

14 A. K. Shiau, D. Barstad, J. T. Radek, M. J. Meyers, K. W. Nettles, B. S. Katzenellenbogen, J. A. Katzenellenbogen, D. A. Agard and G. L. Green, *Nat. Struct. Biol.*, 2002, **9**, 359–364.

15 B. R. Henke, T. G. Consler, N. Go, R. L. Hale, D. R. Hohman, S. A. Jones, A. T. Lu, L. B. Moore, J. T. Moore, L. A. Orband-Miller, R. G. Graham Robinett, J. Shearin, P. K. Spearing, E. L. Stewart, P. S. Turnbull, S. L. Weaver, S. P. Williams, G. B. Wisely and M. H. Lambert, *J. Med. Chem.*, 2002, **45**, 5492–5505.

16 J. Shen, C. F. Tan, Y. Y. Zhang, X. Li, W. H. Li, J. Huang, X. Shen and Y. Tang, *J. Med. Chem.*, 2010, **53**, 5361–5365.

17 S. Martín-Santamaría, J. J. Rodríguez, S. de Pascual-Teresa, S. Gordon, M. Bengtsson, I. Garrido-Laguna, B. Rubio-Viqueira, P. P. López-Casas, M. Hidalgo, B. de Pascual-Teresa and A. Ramos, *Org. Biomol. Chem.*, 2008, **6**, 3486–3496.

18 A. M. Ramos, J. J. Rodríguez, S. Martín-Santamaría, B. de Pascual-Teresa, M. Hidalgo, P. P. López-Casas and B. Rubio-Viqueira, *España, Patente de Invención ES* P200801961, 2008.

19 K. F. Arcaro, Y. Yang, D. D. Vakharia and J. F. Gierthy, *J. Toxicol. Environ. Health, Part A*, 2000, **59**, 197–210.

20 M. J. Frisch, G. W. Trucks, H. B. Schlegel, G. E. Scuseria, M. A. Robb, J. R. Cheeseman, J. Montgomery, J. A. T. Vreven, K. N. Kudin, J. C. Burant, J. M. Millam, S. S. Iyengar, J. Tomasi, V. Barone, B. Mennucci, M. Cossi, G. Scalmani, N. Rega, G. A. Petersson, H. Nakatsuji, M. Hada, M. Ehara, K. Toyota, R. Fukuda, J. Hasegawa, M. Ishida, T. Nakajima, Y. Honda, O. Kitao, H. Nakai, M. Klene, X. Li, J. E. Knox, H. P. Hratchian, J. B. Cross, V. Bakken, C. Adamo, J. Jaramillo, R. Gomperts, R. E. Stratmann, O. Yazyev, A. J. Austin, R. Cammi, C. Pomelli, J. W. Ochterski, P. Y. Ayala, K. Morokuma, G. A. Voth, P. Salvador, J. J. Dannenberg, V. G. Zakrzewski, S. Dapprich, A. D. Daniels, M. C. Strain, O. Farkas, D. K. Malick, A. D. Rabuck, K. Raghavachari, J. B. Foresman, J. V. Ortiz, Q. Cui, A. G. Baboul, S. Clifford, J. Cioslowski, B. B. Stefanov, G. Liu, A. Liashenko, P. Piskorz, I. Komaromi, R. L. Martin, D. J. Fox, T. Keith, M. A. Al-Laham, C. Y. Peng, A. Nanayakkara, M. Challacombe, P. M. W. Gill, B. Johnson, W. Chen, M. W. Wong, C. Gonzalez and J. A. Pople, *GAUSSIAN 03 (Revision C.02)*, Gaussian, Inc., Wallingford, CT, 2004.

21 R. Huey, G. M. Morris, A. J. Olson and D. S. Goodsell, *J. Comput. Chem.*, 2007, **28**, 1145–1152.

22 R. A. Friesner, J. L. Banks, R. B. Murphy, T. A. Halgren, J. J. Klicic, D. T. Mainz, M. P. Repasky, E. H. Knoll, M. Shelley, J. K. Perry, D. E. Shaw, P. Francis and P. S. Shenkin, *J. Med. Chem.*, 2004, **47**, 1739–1749.

23 T. A. Halgren, R. B. Murphy, R. A. Friesner, H. S. Beard, L. L. Frye, W. T. Pollard and J. L. Banks, *J. Med. Chem.*, 2004, **47**, 1750–1759.

24 D. A. Case, T. A. Darden, T. E. Cheatham III, C. L. Simmerling, J. Wang, R. E. Duke, R. Luo, R. C. Walker, W. Zhang, K. M. Merz, B. Roberts, B. Wang, S. Hayik, A. Roitberg, G. Seabra, I. Kolossváry, K. F. Wong, F. Paesani, J. Vanicek, J. Liu, X. Wu, S. R. Brozell, T. Steinbrecher, H. Gohlke, Q. Cai, X. Ye, J. Wang, M.-J. Hsieh, G. Cui, D. R. Roe, D. H. Mathews, M. G. Seetin, C. Sagui, V. Babin, T. Luchko, S. Gusarov, A. Kovalenko and P. A. Kollman, *AMBER 11*, University of California, San Francisco, 2010.

25 J. P. Ryckaert, G. Ciccotti and H. J. C. Berendsen, *J. Comput. Phys.*, 1977, **23**, 327–341.

26 T. Darden, D. York and L. Pedersen, *J. Chem. Phys.*, 1993, **98**, 10089–10092.

